Chinese Journal of
POLYMER SCIENCE

ARTICLE

https://doi.org/10.1007/s10118-021-2530-2
Chinese J. Polym. Sci. **2021**, *39*, 745–755

Melting and Annealing Peak Temperatures of Poly(butylene succinate) on the Same Hoffman-Weeks Plot Parallel to T_m=T_c Line

Zhi-Ning Xie[a], Hai-Mu Ye[b], Tong Chen[a], Tian-Ze Zheng[a], Jun Xu[a*], and Bao-Hua Guo[a*]

[a] *Advanced Materials Laboratory, Department of Chemical Engineering, Tsinghua University, Beijing 100084, China*
[b] *Department of Materials Science and Engineering, College of New Energy and Materials, China University of Petroleum, Beijing 102249, China*

Electronic Supplementary Information

Abstract The crystallization and melting behavior of polymers is of theoretical importance. In this work, poly(butylene succinate) (PBS) was selected as an example to study such behavior at low supercooling *via* introduction of the extended-chain crystal (ECC) of the same polymer as nucleating agent. The crystallization of PBS with its ECC as nucleating agent in a wide temperature range (90–127 °C) and the following melting behavior were studied. It is revealed that the melting point (T_m, for T_c≥113 °C) and the annealing peak temperature (T_a, for T_c=90–100 °C) show similar asymptotic behavior. Both T_m and T_a approach to a value of *ca*. 3.3 °C higher than the corresponding T_c when the crystallization time t_c approaches the starting point. That is to say, the Hoffman-Weeks plot is parallel to T_m=T_c line. The crystallization line became parallel to the melting line when PBS was crystallized at T_c higher than 102 °C. Based on these results, we propose that the parallel relationship and the intrinsic similarity between the T_a and the T_m observed at the two ends of the T_c range could be attributed to the metastable crystals formed at the beginning of crystallization.

Keywords Polymer crystallization; Melting temperature; Hoffman-Weeks plot; Stabilization mechanism; Baby crystal

Citation: Xie, Z. N.; Ye, H. M.; Chen, T.; Zheng, T. Z.; Xu, J.; Guo, B. H. Melting and annealing peak temperatures of poly(butylene succinate) on the same Hoffman-Weeks plot parallel to T_m=T_c line. *Chinese J. Polym. Sci.* **2021**, *39*, 745–755.

INTRODUCTION

The crystallization and melting behavior of polymers is of theoretical importance. A comprehensive understanding of the mechanism should be based on a temperature window of crystallization as wide as possible. In the early days, most studies focused on the polymer lamellar crystals crystallized at high supercooling. Crystallization of polymer at low supercooling and the subsequent melting behavior used to be predicted by extrapolation of the results at high supercooling. The acquisition of the equilibrium melting point (T_m^0) is among the examples. In previous reports, T_m^0 used to be acquired by linear extrapolation of Hoffmann-Weeks plot[1–5] or Gibbs-Thomson Equation.[6,7] However, previous studies have shown that the crystallization and melting behavior at low supercooling is different from that at intermediate and high supercooling, and simple extrapolation would lead to mis-prediction. For example, change from Regime II to Regime I of crystal growth of poly(butylene succinate) (PBS) was reported by Tang *et al.*[8] at 108 °C, close to the ordinary melting point of PBS (~114 °C). Acquisition of T_m^0 *via* linear extrapolation of Hoffmann-Weeks plot is another example that may lead to mis-prediction. It was reported by Xu *et al.*[5] that the slope of Hoffman-Weeks plot for PBS shifted from 0.6 to 1 at 111 °C. It meant that the T_m-T_c curve became parallel with T_m=T_c at low supercooling, thus extrapolation of results at high supercooling could not be applied to obtain T_m^0. Recently, the thermal Gibbs-Thomson equation was proposed by Toda *et al.*,[9,10] which offered an alternative approach to acquire T_m^0 with the assumption that the linear crystallinity determined by the SAXS methods is equal to the bulk crystallinity determined by DSC.

Apart from the discovery mentioned above, there are still some issues not fully understood. One is the stabilization mechanism of the lamellar crystals. Strobl proposed a model that native crystals form through a pathway of metamorphic phase followed by stabilization *via* thickening and transformation to a more stable phase.[11–15] Xu *et al.* recently showed that the native crystals might be stabilized by widening at low supercooling, or by both widening and coalescence at high supercooling.[5] The work by Lv *et al.* further indicated that the stability of lamellae in the isothermally crystallized sample was different.[16] Another question is about the origin of the annealing peak, which has been attributed to different mechanisms, such as rigid amorphous fraction,[17–21] pseudo-crystalline phase,[22] secondary crystallization,[23–26] *etc*. The nature of the annealing peak is still under debate.

* Corresponding authors, E-mail: jun-xu@tsinghua.edu.cn (J.X.)
E-mail: bhguo@mail.tsinghua.edu.cn (B.H.G.)

Received October 28, 2020; Accepted November 23, 2020; Published online December 11, 2020

Therefore, the study of crystallization and melting behavior of polymers at low supercooling is essential and would deepen our understanding on the crystallization mechanism. In recent years, with the development of fast DSC, studies on the crystallization and melting behavior of polymers at low supercooling have been reported.[9,10,27,28] With the aid of this technique, reorganization of originally formed crystals could be avoided so that the melting point just a few degrees Celsius above T_c, could be clearly shown. In addition, a Hoffman-Weeks plot parallel with T_m=T_c curve was observed.[29]

Apart from fast DSC method, application of a heterogeneous yet effective nucleating agent (NA) also makes a feasible approach to crystallization at low supercooling. Our previous work reported application of poly(butylene fumarate) (PBF) as an effective nucleating agent for poly(butylene succinate) (PBS) to realize crystallization of PBS at low supercooling.[5] The advantage of this approach is that heterogeneous NAs would not interfere the melting behavior of the matrix. However, in some cases, the NAs might itself participate in the secondary nucleation of the matrix, as was previously reported by Tang *et al*.[8] and Ye *et al*.[4,30]

Extended-chain crystal (ECC) of the same polymer can be adopted as self-seeds to enhance primary nucleation. Recently, Ye *et al*. reported a green and massive production of the ECC of PBS.[31,32] In this work, we would like to adopt the ECC of the same polymer as nucleating agent to study crystallization at low supercooling and the melting behavior of such crystallized samples. ECC samples of PBS were partially melted and the remaining small amount of ECC worked as nucleating agents during the following isothermal crystallization, which is similar to the previous self-seeding method. But the difference is that now the ECC crystals act as seeds for crystallization of the folded-chain crystals (FCC). Crystallization of the melt with presence of ECC as nucleating agent at intermediate and low supercooling was then investigated. The ECC seeds would not interfere the melting behavior of FCC crystals formed during isothermal crystallization, since the two have quite different melting points. In addition, there is no need of considering polymorphism of PBS during quiescent melt crystallization,[2,33–36] avoiding unnecessary concerns. As a result, we could study the melting behavior of PBS FCC isothermally crystallized at both high and low supercooling. Our observation that the melting temperature and the annealing peak temperatures line in the same Hoffman-Weeks plot with a slope of 1 suggests the probably same near-equilibrium origin of the two phenomena.

EXPERIMENTAL

Materials

The ECC of PBS was fabricated by the previously reported method.[31,32] The ECC applied in this work had a T_m of 135.3 °C, 22 °C higher than that of the folded-chain crystal (FCC) of PBS (113.5 °C). The melting enthalpy (ΔH_m) of ECC was 107.3 J/g, indicating a degree of crystallinity of 97% if we refer to the ΔH_m of 100% crystalline PBS at 110.3 J/g.[37] Selection of this value is based on the study of Ye *et al*.[32]

Gel Permeation Chromatography (GPC)

The number-average molecular weight (M_n) and PDI of PBS before and after fabrication of ECC were measured by GPC (Waters 2695) at 35 °C. The facility is equipped with a differential refractometer detector (Waters 2414 RI Detector) and a laser light scattering detector (WYATT TREOS II). Chloroform (HPLC grade) was used as mobile phase, and a flow rate of 1 mL/min was applied. PBS ECC is hardly dissolvable in chloroform, thus PBS ECC was first treated at 160 °C, and then quenched to room temperature as long as melting was completed. Samples (*ca*. 10.00 mg, original PBS before fabrication of ECC, Showa Denko company; and molten ECC) were dissolved in 2000 μL of chloroform. M_n and PDI of PBS before fabrication of ECC are 6.2×10^4 and 1.17, and those of PBS after fabrication of ECC are 4.1×10^4 and 1.27, respectively.

Differential Scanning Calorimetry (DSC)

Shimadzu DSC-60 was applied for DSC characterization. *Ca*. 2.00 mg of sample was carefully sealed in an aluminum pan, and an empty pan was utilized as reference. The temperature changing rate (β) was 10 K/min if not specifically declared. All scanning procedures were carried out in nitrogen atmosphere (50 mL/min) to prevent any oxidation or degradation.

Self-seeding Procedure of ECC

The temperature profile of the self-seeding method is plotted in Fig. 1. ECC samples were melted at T_s for different periods of time (t_s). The fraction of remaining ECC could be tailored by adjusting T_s (described in detail in the section ECC as seeds *via* partial melting). The samples were cooled to room temperature and then heated to obtain the melting enthalpy of remaining ECC, from which we calculated the quantity of remaining ECC (profile (a) in Fig. 1).

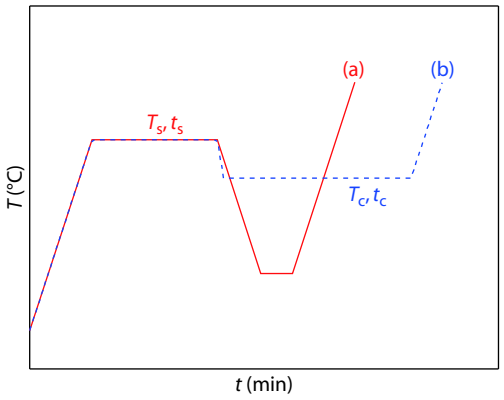

Fig. 1 Temperature profile applied in this work. (a) ECC was treated at T_s=126–136 °C for t_s=2–60 min to melt most of the sample while a small amount of ECC survived. The sample was cooled and then heated. This heating process is to calculate the amount of ECC remaining after self-seeding process. (b) Isothermal crystallization of PBS at T_c=90–127 °C for t_c ranging from a few minutes to 72 h after self-seeding of ECC. After crystallization, the samples were directly heated, so that the melting enthalpy of crystals formed could be calculated.

Isothermal Crystallization

PBS ECC was first treated at T_s for self-seeding, and then the sample was quenched to the isothermal crystallization temperatures T_cs, ranging from 90 °C to 127 °C (profile (b) in Fig. 1). Three different protocols were applied (Table 1).

https://doi.org/10.1007/s10118-021-2530-2

Table 1 Protocols applied in PBS isothermal crystallization.

T_c (°C)	T_s (°C)	Weight percent of ECC during isothermal crystallization	t_c
90–102	160	0	Up to 16 h
104–111	136	0.1%	Up to 8 h
113–127	134	10%	Up to 72 h

For crystallization at T_c=90–102 °C, no ECC was necessary. At these T_cs, crystallization of PBS took place at considerable rate, and the presence of ECC would lead to crystallization during quenching. Therefore, in order to ensure that all crystallization happened during isothermal crystallization, no ECC seeds were left in the samples when PBS was crystallized at 90–102 °C. For crystallization at 104–111 °C, 0.1 wt% ECC crystals were left in PBS by treatment of ECC at T_s=136 °C, so that melt crystallization could be accelerated by the remaining ECC. The lower concentration of ECC (compared with that applied when T_c≥113 °C) was again for the purpose that all crystallization took place in the isothermal process, and no crystallization occurred during quenching. When PBS was crystallized at T_c≥113 °C, *ca.* 10% ECC survived after self-seeding treatment at T_s=134 °C.

Incorporation of seeds (ECC) would significantly shorten the induction period due to acceleration of primary nucleation. However, what we are interested is the result of secondary nucleation at each T_c. The seeds would not participate in secondary nucleation. Therefore, the data and results could be compared.

PBS was isothermally crystallized at each temperature T_c for time t_c ranging from a few minutes to several hours, so that the change in T_m and melting enthalpy (ΔH_m, calculated by integration of DSC curve) of crystals during crystallization could be obtained.

Small Angle X-ray Scattering (SAXS)

The samples were sealed in a mini-chamber formed by an O-ring (inner diameter *ca.* 5 mm) sandwiched by polyimide (Kapton) films. The samples then underwent the same isothermal crystallization procedure on Linkam (T96S and LNP96S). SAXS measurements were carried out on a Xeuss 2.0 SAXS/WAXS system (Xenocs, France) with an X-ray wavelength of 0.154 nm. 2D SAXS patterns were collected *via* a Pilatus detector (Switzerland), having a resolution of 487×619 pixels (each pixel size of 172 μm × 172 μm). The 2D patterns were further integrated to obtain 1D scattering intensity distributions (*I*-*q* curves), which were corrected to remove sample absorption and background scattering from air. The sample-to-detector distance was *ca.* 2500 mm, corresponding to an effective range of the scattering vector $q = \frac{4\pi}{\lambda}\sin\left(\frac{\theta}{2}\right)$ of 0.042–2.21 nm^{-1}, in which θ is the scattering angle. The distance was determined by a silver behenate ($AgC_{22}H_{43}O_2$) standard. SAXS patterns were collected after 20 min exposure. The 1D correlation function was derived from the Fourier transform of the Lorentz corrected SAXS profile. The lamellar thickness L_c, amorphous layer thickness L_a and long period L_p can be deduced.[14,38,39] The average long period L_p is determined from the first maximum of the correlation curve. The thickness of the thinner layer l_1 was given by the intersection of the straight line extended from the self-correlation triangle and the baseline (Fig. S2 in the electronic supplementary information, ESI), and that of the thicker layer l_2 was calculated by $l_2 = L_p - l_1$. The thinner layer was attributed to the lamellar core thickness L_c, and was supported by the recent work of Zhang *et al.*,[40] in which L_p increased as the number of non-crystallizable units increased in poly(butylene succinate-*co*-butylene 2-methylsuccinate) copolymers, and increase of long period was contributed by the thicker layer while the thickness of thinner layer remained almost unchanged, indicating that the thinner layer should reflect L_c, while the thicker layer should reflect the thickness of amorphous layer L_a.

RESULTS AND DISCUSSION

ECC as Seeds *via* Partial Melting

The thermal properties of ECC applied in this work are displayed in Fig. 2. ECC was treated at 160 °C for 5 min, cooled to room temperature, and then subjected to the 2nd heating. The first heating DSC curve shows that PBS ECC has a melting point of 135.3 °C. The second heating curve gives a melting peak at 113.5 °C, which is the normal melting peak temperature of recrystallized PBS folded-chain crystals (FCC). Disappearance of the melting peak at around 135 °C indicates that no ECC

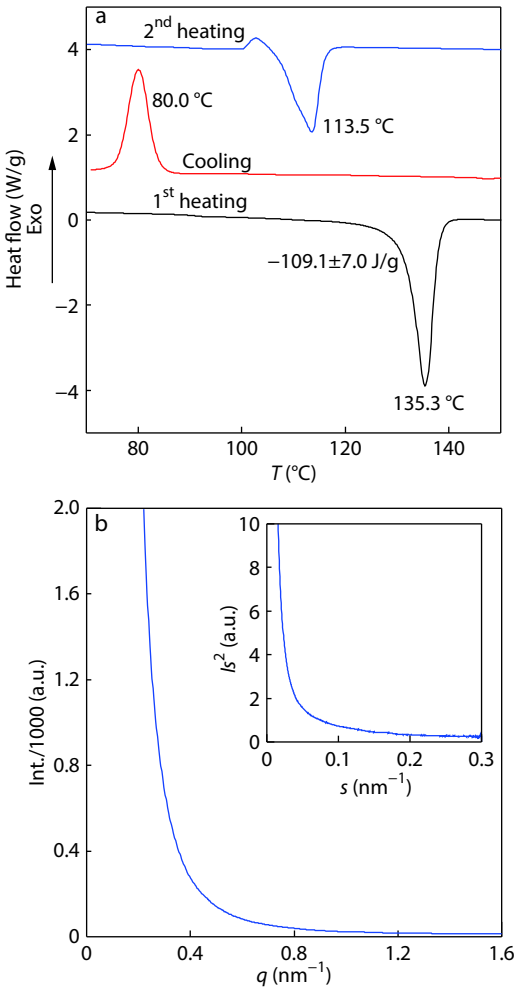

Fig. 2 (a) DSC curves of the 1st heating, cooling and the 2nd heating process of PBS ECC; (b) SAXS profiles of PBS ECC, before and after (inset, $s = q/2\pi$) Lorentz correction.

https://doi.org/10.1007/s10118-021-2530-2

remained after treatment at 160 °C for 5 min (Fig. 2a). SAXS scanning of ECC sample reveals that ECC produces no peak in the observed curve (Fig. 2b). Later, PBS would be crystallized at various T_c before subjected to SAXS characterization in order to explore the lamellar thickness at each T_c. For crystallization at T_c higher than 102 °C, a small amount of ECC would be presented as nucleating agent *via* self-seeding. The results in Fig. 2(b) show that ECC in the sample would not interfere with the results of SAXS scanning.

Incorporation of ECC into PBS was realized *via* partial melting of PBS ECC samples. We did not apply the other methods based on the following concerns:

(1) Solution blending. Although ECC of PBS is hard to dissolve, solution blending aided *via* ultrasonication might still damage ECC.

(2) Mechanical blending. Exposure to high temperature, torque and oxygen is involved. Degradation of PBS might occur. Any fluctuation in temperature during blending would result in total elimination of ECC, which is the last thing desired.

(3) Blending might result in double-peak distribution of molecular weight in the system, which would make the system complex.

Due to these concerns, the self-seeding method in Fig. 2 was applied. Part of ECC was melted by treating PBS ECC samples at T_s for t_s. The following melt crystallization would be strongly enhanced by the seeds (remaining ECC).

The quantities of seeds (ECC) could be controlled by adjusting temperature of self-seeding (T_s). Influences of T_s and t_s on quantities of ECC are shown in Figs. S1 and S2 (in ESI).

It is revealed in Fig. S2 (in ESI) that t_s shows almost no influence on the quantities of seeds. Considering the time of exposure applied in SAXS characterization, t_s of 20 min was selected. ECC was treated at T_s=126–136 °C for 20 min (Fig. 1a). The second heating DSC curves are shown in Fig. S1(a) (in ESI). The quantities of remaining ECC were calculated by $\frac{H_{m,after}}{H_{m,before}}$. The quantities of seeds would be *ca.* 10%, 1% and 0.1% after treating ECC at 134, 135 and 136 °C, respectively. No ECC would remain in the system when T_s exceeds 137 °C.

The controlling of quantities of seeds is examined by the standard deviation (error bars in Figs. S1b and S2 in ESI, n=5). The controlling is repeatable considering the relatively small error bar (maximum relative deviation 13%, at T_s= 134 °C, only data of t_s=20 min compared) and the system error of DSC.

We have to make sure that ECC remains in the system while at the same time no pre-ordering exists in molten ECC. ECC was treated at 160 °C for 5 min to fully melt before quenched to 90 °C and crystallized at 90 °C for 1 h. The crystallized PBS FCC was then treated at T_s=117–138 °C for t_s=20 min. The samples were cooled at 10 K/min after treatment, and peak temperature of crystallization during cooling (T_{cl}) is presented in Fig. S1(b) (in ESI). After treating FCC of PBS at T_s>130 °C, T_{cl} in the following cooling process stays at *ca.* 80 °C. Therefore, no pre-ordering would exist in melted PBS after treatment at T_s>130 °C, otherwise T_{cl} should increase.

Based on the above results, the incorporation of seeds by partial melting of PBS ECC is a feasible method for studying the crystallization of PBS at high T_cs.

Isothermal Crystallization

Isothermal crystallization of PBS was carried out in a wide range of temperatures from 90 °C (high supercooling) to 127 °C (at vicinity of 135 °C, the melting point of ECC). The following melting curves of the isothermally crystallized PBS are shown in Fig. 3. When PBS was crystallized at 90–100 °C, the annealing peak (T_a) and two melting endotherms (T_m and $T_{m,re}$) were observed during the subsequent heating. T_a–T_c curve is parallel with T_m=T_c and could be expressed by Eq. (1):

$$T_a = T_c + \delta_a, \quad (1)$$

The melting endotherm with the lower peak temperature (T_m) should be attributed to the originally formed lamellar crystals of PBS. The constant melting temperature, $T_{m,re}$, at ~113 °C results from melting of recrystallized PBS during heating. The assignment of endotherms during heating of PBS had been studied in detail by previous researchers.[41–45] $T_{m,re}$ disappeared when T_c exceeded 102 °C, and T_m gradually increased with rising T_c.

The seeds (ECC) are crucial for crystallization at high T_cs. We firstly examined the crystallization of neat PBS (with no

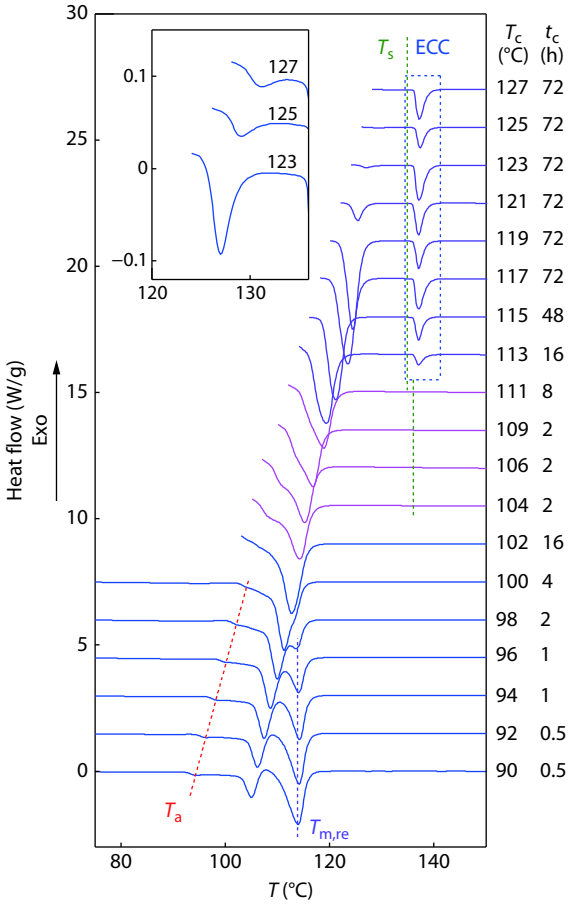

Fig. 3 DSC curves of the second heating after crystallization of PBS at 90–127 °C for t_c ranging from 0.5 h to 72 h. The corresponding t_c was offered at the same time. The color of DSC curves corresponds with the protocols in Table 1. T_s of 160 (blue), 136 (violet) and 134 °C (purple) was applied for crystallization at 90–102, 104–111 and 113–127 °C respectively. The inset shows the small melting peak of FCC PBS *via* magnifying DSC curves of PBS crystallized at 123–127 °C for 72 h.

https://doi.org/10.1007/s10118-021-2530-2

seeds) at 109 °C after elimination of thermal history (treated at 160 °C for 5 min). No crystallization of PBS was observed until t_c reached 16 h (data not shown here). In comparison, when ECC seeds were present by self-seeding of ECC at T_s=136 °C, observable crystallization occurred within 10 min. In addition, crystallization at 115 °C with and without ECC seed was compared. PBS FCC isothermally crystallized at 90 °C was treated at 134 °C for 20 min. No seeds were left after this treatment (Fig. S1b in ESI). The melt was then quenched to 115 °C and kept at 115 °C for 72 h. The process was observed *via in situ* XRD characterization, and no peaks were observed during the whole process, indicating the absence of crystals. In comparison, when ECC seeds existed by treating ECC at 134 °C for 20 min, crystallization at 115 °C was observed within 1 h. The comparisons prove the crucial role of ECC seeds in primary nucleation of isothermal crystallization of PBS at high T_cs.

In order to ascertain the melting endotherm observed after crystallization at above 113 °C, PBS was crystallized at 117 °C for 2 h and directly heated at β=0.5–40 K/min (Fig. 4b). In order to provide reference for the β dependence of melting of original crystals (T_m), that of recrystallized PBS ($T_{m,re}$) and annealing peak (T_a), PBS was isothermally crystallized at 90 °C for 1 h, cooled to room temperature, and then heated at β=1–99 K/min (Fig. 4a). Cooling was involved so that the annealing peak (T_a) could be better observed. T_a would be superimposed with the change of C_p if samples were heated directly after crystallization. The cooling process shows no influence on T_m.

For PBS isothermally crystallized at 90 °C, a monotonic increase in T_m and T_a is observed with increasing heating rate. The endotherm peak temperature that represents melting of recrystallized PBS during heating ($T_{m,re}$) first decreases with increasing β, and starts to increase with β for β>10 K/min. The melting peak of original crystals and recrystallized crystals could well be distinguished before β reached 99 K/min, at which only one melting endotherm could be observed. In addition, T_a is no longer observable at β=99 K/min.

For PBS crystallized at 117 °C for 2 h, monotonic increase in peak temperature of the melting endotherm is observed as β increases. It is demonstrated that this endotherm should be attributed to melting of the original crystals formed during isothermal crystallization. If the original lamellae had experienced re-organization during heating, the melting peak temperature T_m should first decrease with arising heating rate. In fact, this is not the case, so we could preclude the possibility of reorganization before T_m during DSC heating.

Variation of Melting Temperature and Enthalpy with Isothermal Crystallization Time

It is pointed out in the section Isothermal Crystallization that T_m varies with both β and t_c. It has also been reported that T_a would change with the logarithm of t_c,[24–26] indicating that δ_a in Eq. (1) would also depend on t_c. In order to clarify such dependence, PBS was crystallized at T_c of 96–127 °C for t_c varying from a few minutes to 72 h (temperature profile (b) in Fig. 1). The evolution of T_m and ΔH_m, T_a, and the gap between T_m/T_a and T_c during crystallization is illustrated in Fig. 5, Fig. S5 (in ESI) and Fig. 6, respectively. ΔH_m is calculated by integration of DSC curves.

The primary and secondary stages of crystallization can be well illustrated in Fig. 5. In the primary stage, a sigmoidal curve is observed in the ΔH_m-lgt_c plot. The primary stage corresponds to the period in which spherulites gradually grew and filled the screen in POM observation. In the secondary stage, ΔH_m increases linearly with lgt_c. The secondary stage corresponds to crystal perfection, accompanied with the formation of inter-lamellar crystals.[9,10] The transition from primary to secondary stage of crystallization at T_c=104 and 111 °C is marked by arrows in Fig. 5(b).

T_m seems to approach a plateau value as t_c approaches 0. As crystallization proceeds, an obvious increase in T_m with lgt_c occurs, which coincides with that in ΔH_m. For crystallization at T_c≤104 °C, T_m finally levels off as long as crystallization proceeds into the secondary stage (Figs. 5a and 5b), and $T_{m,re}$ evolves in almost the same way as T_m (T_c=96–98 °C, the open and semi-filled symbols in Fig. 5a). For crystallization at T_c≥

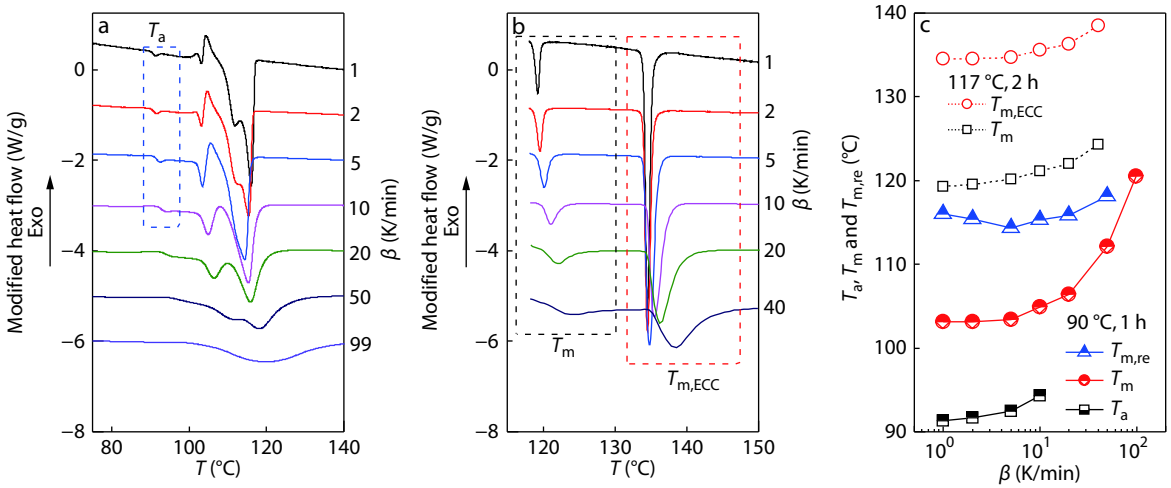

Fig. 4 (a) PBS was isothermally crystallized at 90 °C, and then heated at heating rate (β) ranging from 1 K/min to 99 K/min. (b) PBS was crystallized at 117 °C for 2 h, and then heated at β=1–40 K/min. The DSC curves in (a) and (b) were modified by multiplying a factor 10/β. (c) The melting points and T_a of PBS isothermally crystallized at 117 °C (hollow symbols, prepared by self-seeding of ECC) and at 90 °C (semi-filled symbols). Only the highest $T_{m,re}$ was recorded.

https://doi.org/10.1007/s10118-021-2530-2

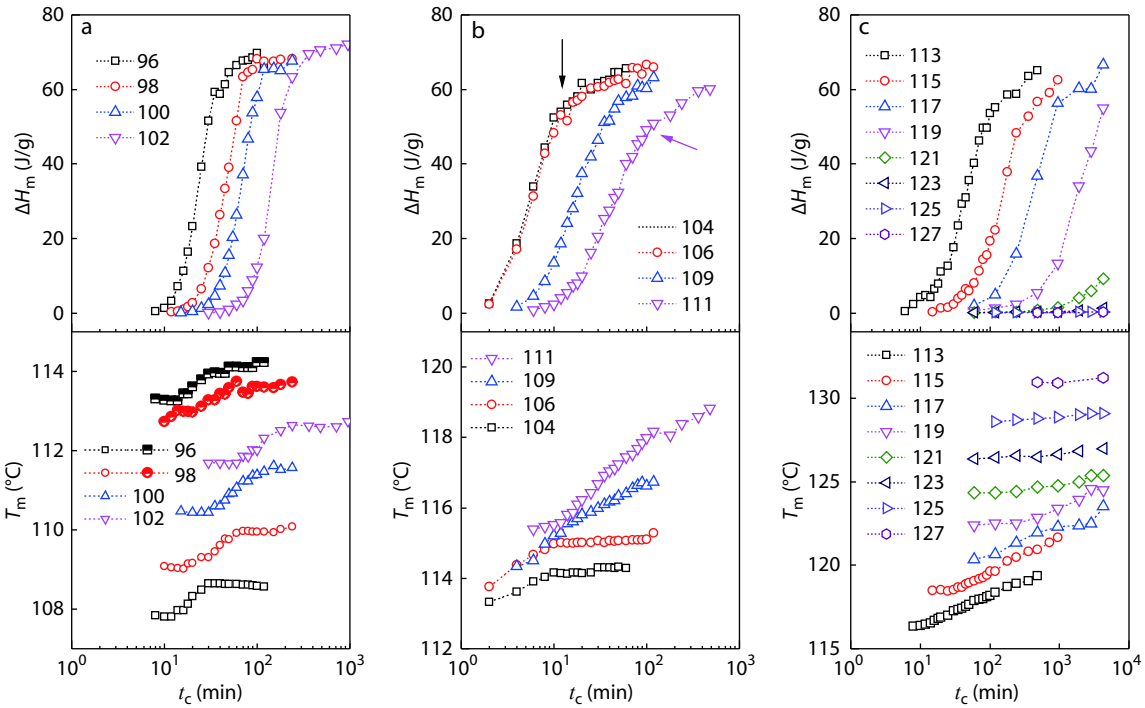

Fig. 5 The evolution of T_m and ΔH_m during crystallization. Three different protocols (exhibited in Table 1) were applied: (a) crystallization at 96–102 °C with T_s=160 °C (no ECC remained), (b) crystallization at 104–111 °C with a T_s of 136 °C (0.1 wt% ECC remained), and (c) crystallization at 113–127 °C with a T_s of 134 °C employed (10 wt% ECC remained). The open symbols refer to the melting point of the original crystals, and the semi-filled symbols in (a) refer to $T_{m,re}$ of PBS crystallized at 96 and 98 °C. Transition from primary to secondary stage of crystallization at T_c=104 and 111 °C was marked by arrows in (b).

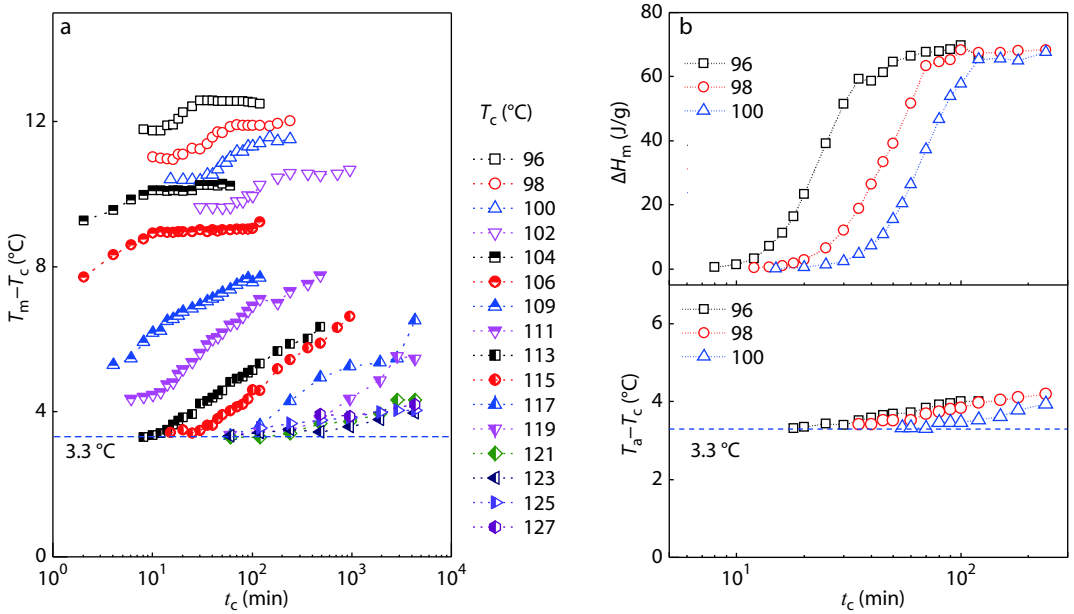

Fig. 6 (a) Semilogarithmic plot of (T_m-T_c) at T_c=96–127 °C against t_c and (b) semilogarithmic plot of ΔH_m and (T_a-T_c) at T_c=96–100 °C against t_c. (T_m-T_c) at $T_c \geq 113$ °C and (T_a-T_c) at $T_c \leq 100$ °C approach an asymptote at ~3.3 °C when t_c approaches 0.

104 °C, T_m continues to grow obviously with the logarithm of t_c in the secondary stage.

The increase in T_m might possibly result from the thickening of lamellae during isothermal crystallization.[46–48] In order to examine the evolution of lamellar thickness during crystallization, an *in situ* SAXS characterization was carried out at 117.5 °C. The results are shown in Fig. S4 (in ESI). In the first 12 h, no increase in L_c is observed, while the melting point could have increased by *ca.* 2 °C (Fig. 5c) in this period. Therefore, the increase of T_m might result from the increase of lamellar width rather than thickness.

The evolution of T_a for crystallization at 96–100 °C was ex-

https://doi.org/10.1007/s10118-021-2530-2

amined *via* the 2nd derivative of DSC heating curves. Results are exhibited in Fig. S5 (in ESI). The position of the annealing peak was determined by the 1st maximum of 2nd derivative. T_a gradually shifts to higher temperature, very similar to the trend of the melting peak temperature of original crystals, which is in accordance with the previous reports.[23–26]

Based on these results, the gap between T_a and T_c (δ_a in Eq. 1) and that between T_m and T_c are plotted in Fig. 6. Fig. 6(a) shows that the gap gradually increases with prolonged t_c, and decreases with increasing T_c for T_c≤111 °C. At T_c≥113 °C, however, all (T_m–T_c) values approach *ca.* 3.3 °C at the starting point of crystallization. It is interesting to find out in Fig. 6(b) that the (T_a–T_c) values also approach the same value at the start of crystallization when PBS was crystallized at T_c≤100 °C.

The plateau values of T_a and T_m when t_c approaches the starting point of crystallization are denoted as $T_{a,ini}$ and $T_{m,ini}$, respectively. $T_{a,ini}$ and $T_{m,ini}$ are read from the results in Figs. 5 and 6, as illustrated in Fig. 7. The original T_m-T_c curve is shown in Fig. S6 (in ESI).

The plot exhibits 2 slopes described by Eq. (2):

$$T_{m,ini} = \begin{cases} aT_c + b & (T_c \le 102\ ^\circ\mathrm{C}) \\ T_c + \delta & (T_c \ge 113\ ^\circ\mathrm{C}) \end{cases} \quad (2)$$

When T_c≤102 °C, $T_{m,ini}$-T_c curve has a slope (a) of 0.65 and the linear extrapolation gives an intersection with T_m=T_c line at 129.6 °C (T_x in Fig. 7). It has been reported previously that linear extrapolation of Hoffmann-Weeks plot of PBS intersected with T_m=T_c at 127–140 °C.[1–5] Therefore, the result of our linear extrapolation is in accordance with previous reports. However, an obvious change in a occurs at 113 °C. a shifts from 0.65 to 1.00, resulting in a T_m-T_c curve parallel with T_m=T_c line, *i.e.* a Hoffman-Weeks plot with slope of 1. At large supercooling, the slope of Hoffman-Weeks plot is below 1, due to which linear extrapolation of H-W plot to intersect with T_m=T_c line was available in previous reports.[1–5] The Hoffman-Weeks plot parallel to T_m=T_c line at low supercooling means that linear extrapolation to intersect with T_m=T_c line is no longer possible. The parallel relationship between the Hoffman-Weeks plot and T_m=T_c line in this work is in accordance with our previous report,[5] in which the shift of a to 1 was observed at

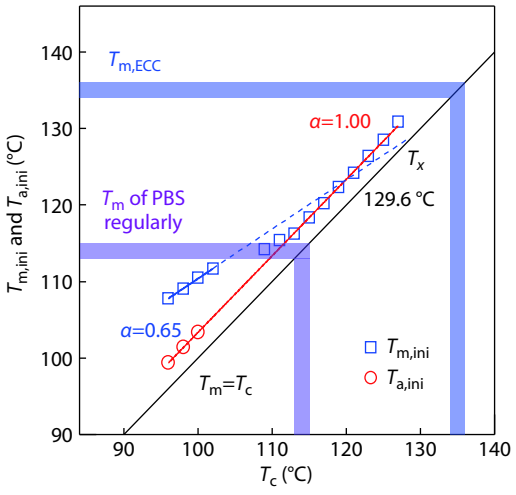

Fig. 7 Plot of $T_{m,ini}$ and $T_{a,ini}$ versus T_c. $T_{m,ini}$ (T_c≥113 °C) and $T_{a,ini}$ (T_c≤100 °C) show parallel relationship with T_c.

110 °C. However, crystallization and melting behavior of PBS at T_c higher than 113 °C was not further explored in the previous work. In this work we are able to extend crystallization into lower supercooling, and the parallel relationship between T_m and T_c extends to up to T_c=127 °C. In addition, the effect of crystallization time on melting point was not considered in our previous work.[5] The T_m-T_c curve parallel with T_m=T_c line has also been observed in PEEK,[27,49] PCL,[50] PA6,[51] PBT[28,52] and PPS.[53] The parallel relationship between T_m and T_c indicates that T_m^0 could not be obtained *via* linear or nonlinear extrapolation of Hoffman-Weeks plot.

It is noteworthy that both $T_{m,ini}$-T_c curve (T_c≥113 °C) and $T_{a,ini}$-T_c curve (T_c≤100 °C) lie on the same line parallel to T_m=T_c line (R^2>0.99), exhibiting a parallel relationship in a wide T_c range. This observation indicates that the annealing peaks appearing at low T_c and the melting peaks at high T_c might have intrinsic similarity. The similarity will be discussed in the following.

Lamellar thickness (L_c) of the isothermally crystallized PBS examined *via* SAXS is given in Fig. 8, Fig. S4 and Table S1 (in ESI). It is revealed in Figs. 8(a) and 8(b) that thicker lamellae are formed at increased T_c. The increase in L_p is more drastic than that in L_c. L_c of PBS crystallized at 123 and 127 °C was unable to be calculated due to low crystallinity and thus weak scattering intensity. DSC scanning of SAXS samples after scattering (Fig. S5 in ESI) proves the existence of crystallized PBS at 123 and 127 °C. Based on these results and the assumption that no lamellar thickening occurs in the heating process, the crystallization line and melting line are drawn, as displayed in Fig. 8(c).

When crystallized at 90–102 °C, the crystallization line is much steeper than the melting line. The lines could have intersected were it not for the abrupt change in the slope of crystallization line at T_c=102 °C. The crystallization line parallels to the melting line at T_c>102 °C. The mechanism of the change in the slope of crystallization line has been discussed by Xu *et al.*[5] The change of slope is proposed due to the different mechanisms of crystal stabilization (decrease of free energy of the crystals). At high supercooling (*i.e.* T_c<102 °C), the metastable crystal nuclei are predominantly stabilized by coalescence of neighbouring nuclei. At low supercooling, the metastable nuclei are stabilized by widening growth.

Discussion

In the above two sections, changes in slope of T_m-T_c curve and the crystallization line are observed. Both T_m–T_c and T_m–T_a gaps approach *ca.* 3.3 °C at the starting point of crystallization. The similarity between T_m at low supercooling and T_a at high supercooling indicates intrinsic similarity.

Crystallization of polymers starts with the formation of metastable crystals, which are just slightly thicker than the thermodynamically predicted minimum thickness (l_c*) so that the crystals could survive.[5] We notice that recently Albrecht *et al.*[29] reported the observation of "original crystals" which melts at temperatures a few degrees Celsius higher than T_c. The metastable crystals have large specific surface area, and have a T_m just a few degrees higher than T_c.

The metastable crystals can be further stabilized by reduction in free energy.[5] When T_c≥113 °C, the sample features great difficulty in nucleation, leading to an extremely low

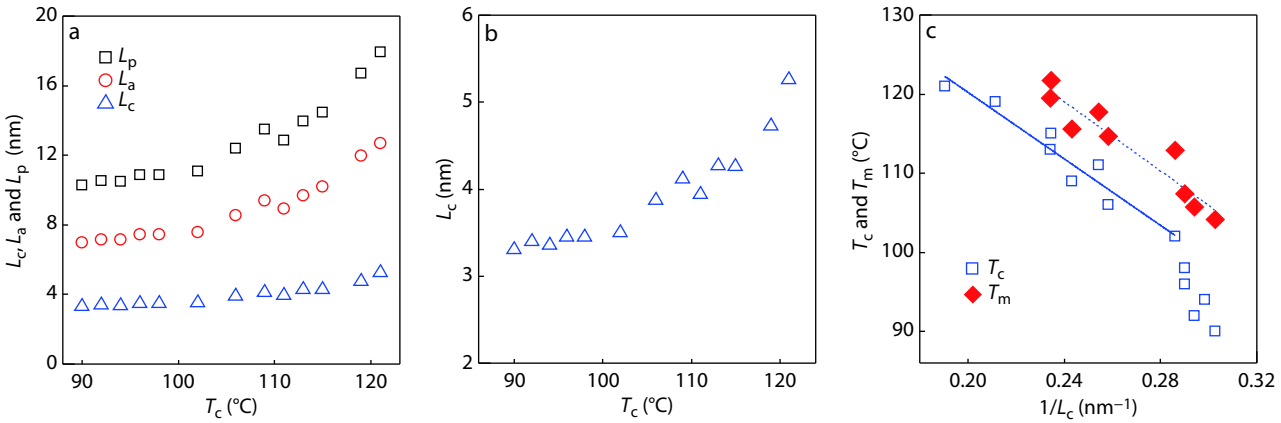

Fig. 8 (a) The lamellar thickness (L_c), the amorphous layer thickness (L_a) and long period (L_p) calculated *via* correlation function. The L_c-T_c plot was magnified and displayed in (b). (c) The crystallization line (open symbols) and melting line (solid symbols).

nucleation density. $T_{m,ini}$ reflects melting point of the metastable crystals formed at the beginning of crystallization (Fig. 9b). The metastable crystals need further stabilization. However, stabilization *via* coalescence is considered impossible due to low nucleation density at low supercooling.[5] Thickening during isothermal crystallization is another possible method of stabilization, which has been reported in polymers like PE, PEO, PCL, *etc*.[46–48] However it has been illustrated in Fig. S4 (in ESI) that the increase in L_c was not observed during isothermal crystallization of PBS. Therefore, the near-equilibrium metastable crystals of PBS at the beginning of crystallization are not yet stabilized. With prolonged time at the isothermal crystallization temperature, they could only be stabilized by continuous attachment of stems during lateral spreading. Growth in lateral size leads to increase in T_m according to Gibbs-Thomson equation.[54] However, the thermal stability of crystals was only improved by a limited amount. One possible reason might be the decreasing length of attached stems.[55]

When T_c≤100 °C, nucleation density is high, thus metastable nuclei coalesce rapidly to form more stable crystals (purple box in Fig. 9a). However, diffusion must be taken into consideration. The chain movement is quickly frozen due to rapid crystallization before some metastable crystals could find their way to coalescence (red box in Fig. 9a). T_a is the result of the remaining unstabilized metastable crystals, which failed to coalesce. The proposition could be supported by the work of Schick *et al.*,[28] in which the melting peak of PBT a few degrees above T_c corresponded to the original crystals. As crystallization proceeds, T_a increases with logarithm of t_c (Fig. 6). The shift to higher temperature was attributed by Marand *et al.* to the decrease in molar conformational entropy of the remaining amorphous fraction.[24] This might be one possible reason and another possible reason may be the perfection of the crystals with time, which both leads to increase of melting point with time.

The stability of remaining metastable crystals may be different. These crystals differing in melting point are continuously melted before fusion of the stabilized crystal (T_m) appears. The crystals with the least stability contribute to the peak at T_a. Therefore, endothermic process continues after the appearance of T_a, resulting in a "step" in DSC curve

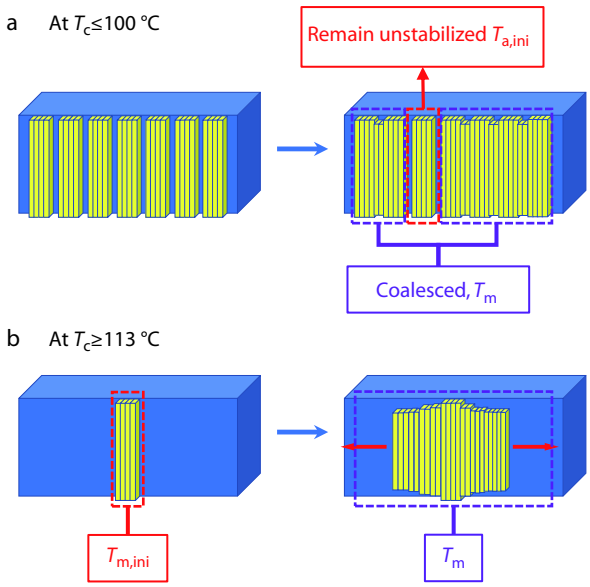

Fig. 9 Schematic showing of the origin of T_a and $T_{m,ini}$. (a) When PBS is crystallized at T_c≤100 °C, nucleation density is high. Multiple metastable crystals are formed at the beginning. Most crystals are stabilized rapidly by coalescence. The system is frozen soon after crystallization, and some metastable crystals remain unstabilized. The unstabilized metastable crystals lead to observation of T_a. (b) When PBS is crystllized at T_c≥113 °C, nucleation density is low. The metastable crystals are stabilized by lateral spreading *via* continuous attaching clusters (red arrows in b). $T_{m,ini}$ reflects the metastable crystals in the beginning of crystallization.

(Fig. 4a). The similar result was reported by Lv *et al. via* step heating DSC procedure. It was observed that the isothermally crystallized PBS crystals melted at various temperatures and no recrystallization occurred during heating after T_c reached 106 °C.[16]

Crystals with varying stability could be discriminated by step-cooling and step-heating process, as shown in Fig. 10. In step-cooling (Fig. 10a), PBS was crystallized at T_c step-wisely decreased from 100 °C to 60 °C (5 °C per step), with t_c at each step fixed for 30 min. Multiple T_as appear in the following heating process, well fitted by Eq. (1). In step-heating process, PBS was isothermally crystallized at 90 °C before being heated

https://doi.org/10.1007/s10118-021-2530-2

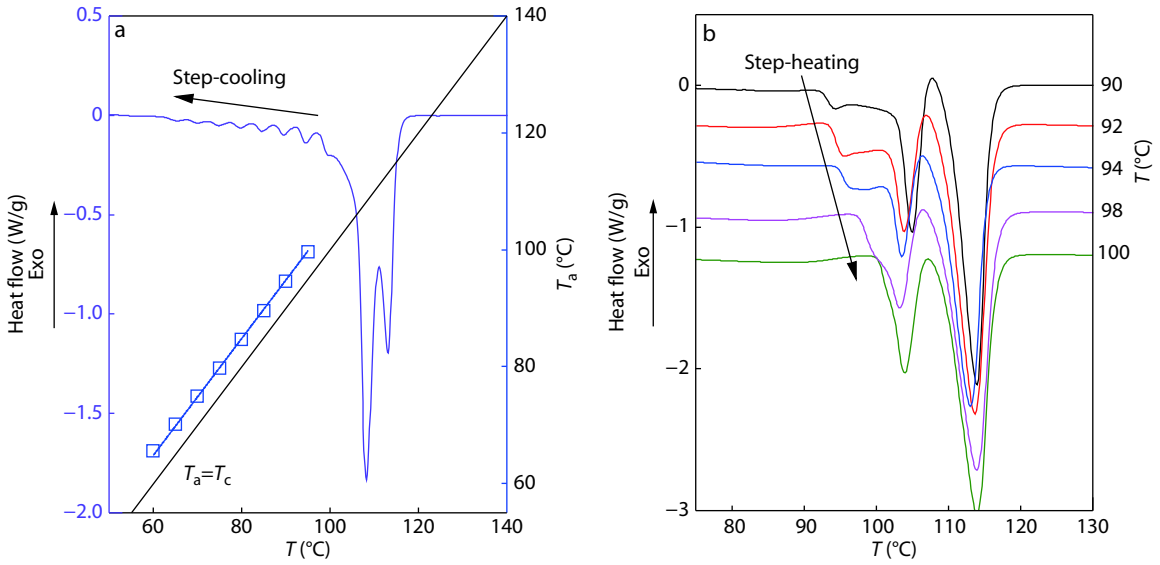

Fig. 10 The annealing peaks in (a) step-cooling and (b) step-heating process.

step-wisely to 92–100 °C (2 °C per step), and held at each step temperature for 20 min. T_a continuously shifts to higher temperature, while T_m remains almost unchanged after the step-heating process. The crystals with the least stability were melted with the increase in $T_{treatment}$. The un-molten crystals either remain unchanged or experience stabilization. The stability of crystals was thus discriminated by the various peaks in step-cooling, and the shift of T_a in step-heating. Interestingly, we notice that Reiter *et al.*[56] reported similar melting phenomenon of crystals confined in the spherical cells formed by the block copolymer, which only had a choice of either melting immediately or undergoing various degrees of reorganization during heating, producing a broad range of melting temperature.

The nature of annealing peak has been investigated in previous references. Some researchers attributed T_a to the devitrification of rigid amorphous fraction (RAF), in which chains are immobilized by the crystalline phase.[17–21] However, it is difficult to accept the proposition that the chains immobilized in RAF are freed while the constraint exerted by the crystalline phase remain unchanged. The results in Fig. 10 also indicate that with step-wisely lowering T_c, multiple T_as could appear. If chains had already been immobilized in the RAF generated at a higher T_c, how could a T_a corresponding to a lowered T_c be formed and observed?

The proposal of pseudo-crystalline phase originates from the increased mechanical strength of PP.[22] Yet the physical image of pseudo-crystalline phase shows no significant difference from that of RAF.

It was also proposed by Marand *et al.* that T_a results from secondary crystallization.[23–26] It is possible that the inserted thinner lamellae might have T_m much lower than the previously formed skeletal thicker lamellae. However, in this work, T_a is observed before crystallization reaches the secondary stage (Fig. 6b). Therefore, it would not be appropriate to attribute T_a to secondary crystals in this work.

Our proposition for the origin of T_a differs from those in previous work in terms of detailed explanations.[17–26] However, all the interpretations rely on certain restrictions leading to observance of T_a, *e.g.* restriction in chain mobility by crystalline phase (RAF and pseudo-crystalline phase),[17–22] and limited space between existing lamellae (secondary crystallization[23–26]).

The observation that the melting temperature and the annealing peak temperatures line in the same Hoffman-Weeks plot with a slope of 1 could thus be explained. Both $T_{a,ini}$ (T_c≤100 °C) and $T_{m,ini}$ (T_c≥113 °C) are the result of the metastable crystals formed at the beginning of crystallization. Such crystals are not observed when PBS was crystallized at 100–106 °C, which could probably be attributed to higher chain mobility and thus less restriction at lifted crystallization temperature. The near-equilibrium crystals are all stabilized under such condition.

CONCLUSIONS

In this work, the isothermal crystallization of PBS covering a wide T_c range from 90 °C to 127 °C *via* self-seeding with ECC as nucleating agent and the following melting behavior were studied. The melting peak temperature T_m at T_c≥113 °C and the annealing peak temperature T_a at T_c≤100 °C show similar asymptotic behavior, approaching to *ca.* 3.3 °C above T_c at the starting point of crystallization (denoted as $T_{m,ini}$ and $T_{a,ini}$). Namely, the plots of $T_{a,ini}$ at high supercooling and $T_{m,ini}$ at low supercooling with T_c are parallel to T_m=T_c line. A shift of the slope (α) of $T_{m,ini}$-T_c curve from 0.65 to 1.00 at T_c=113 °C was observed. SAXS results revealed that the lamellar thickness remained constant during the isothermal crystallization process. Based on the results, we propose that the parallel relationship originates from metastable crystals formed at the beginning of crystallization. Such crystals are at near-equilibrium state and have not yet been stabilized so they melt at temperatures a few degrees Celsius higher than T_c. At T_c≤100 °C, some just formed metastable crystals failed to stabilize *via* coalescence due to quickly frozen chain movement and their melting results in $T_{a,ini}$. When crystallization happens at T_c≥113 °C, the melting point of

https://doi.org/10.1007/s10118-021-2530-2

the metastable crystals at the beginning of crystallization gives $T_{m,ini}$. Since both $T_{m,ini}$ and $T_{a,ini}$ represent crystals at the near-equilibrium and not yet stabilized state, both the $T_{m,ini}$-T_c curve at low supercooling and $T_{a,ini}$-T_c curve at high supercooling are parallel with T_m=T_c line.

Electronic Supplementary Information

Electronic supplementary information (ESI) is available free of charge in the online version of this article at https://doi.org/10.1007/s10118-021-2530-2.

ACKNOWLEDGMENTS

This work was financially supported by the National National Science Foundation of China (Nos. U1862205, 51473085, and 21873054) and Tsinghua University Initiative Scientific Research Program (No. 20194180048). The authors wish to thank Prof. Wei Miao from School of Materials, Tsinghua University, who kindly offers great help in WAXD data analysis. We thank Dr. Ying Lu from Changchun Institute of Applied Chemistry, and Dr. Yu Wang from the Institute of Chemistry Chinese Academy of Sciences, for their valuable advice and discussion in data analyses of SAXS. The authors declare no conflict of interest.

REFERENCES

1 Miyata, T.; Masuko, T. Crystallization behaviour of poly(tetramethylene succinate). *Polymer* **1998**, *39*, 1399–1404.
2 Gan, Z.; Abe, H.; Kurokawa, H.; Doi, Y. Solid-state microstructures, thermal properties, and crystallization of biodegradable poly(butylene succinate) (PBS) and its copolyesters. *Biomacromolecules* **2001**, *2*, 605–13.
3 Park, J. W.; Kim, D. K.; Im, S. S. Crystallization behaviour of poly(butylene succinate) copolymers. *Polym. Int.* **2002**, *51*, 239–244.
4 Ye, H. M.; Tang, Y. R.; Xu, J.; Guo, B. H. Role of poly(butylene fumarate) on crystallization behaviour of poly(butylene succinate). *Ind. Eng. Chem. Res.* **2013**, *52*, 10682–10689.
5 Xu, J.; Heck, B.; Ye, H. M.; Jiang, J.; Tang, Y. R.; Liu, J.; Guo, B. H.; Reiter, R.; Zhou, D. S.; Reiter, G. Stabilization of nuclei of lamellar polymer crystals: insights from a comparison of the Hoffman-Weeks line with the crystallization line. *Macromolecules* **2016**, *49*, 2206–2215.
6 Hoffman, J. D. D., G. T.; Lauritzen, J. I., The rate of crystallization of linear polymers with chain folding. In *Treatise on solid state chemistry*, Hannay, N. B. Ed. Plenum Press, New York, **1976**, Vol. 3.
7 Wunderlich, B., Crystal Melting. In *Macromolecular physics*, Academic Press, New York, **1980**, Vol. 3.
8 Tang, Y. R.; Gao, Y.; Xu, J.; Guo, B. H. How to regulate the isothermal growth rate of polymer spherulite without changing its molecular composition? *CrystEngComm* **2015**, *17*, 6467–6470.
9 Toda, A.; Taguchi, K.; Nozaki, K.; Guan, X. C.; Hu, W. B.; Furushima, Y.; Schick, C. Crystallization and melting of poly(butylene terephthalate) and poly(ethylene terephthalate) investigated by fast-scan chip calorimetry and small angle X-ray scattering. *Polymer* **2020**, *192*, 122303.
10 Toda, A.; Taguchi, K.; Kono, G.; Nozaki, K. Crystallization and melting behaviours of poly(vinylidene fluoride) examined by fast-scan calorimetry: Hoffman-Weeks, Gibbs-Thomson and thermal Gibbs-Thomson plots. *Polymer* **2019**, *169*, 11–20.
11 Strobl, G. Colloquium: laws controlling crystallization and melting in bulk polymers. *Rev. Mod. Phys.* **2009**, *81*, 1287–1300.
12 Strobl, G. Crystallization and melting of bulk polymers: new observations, conclusions and a thermodynamic scheme. *Prog. Polym. Sci.* **2006**, *31*, 398–442.
13 Strobl, G. From the melt *via* mesomorphic and granular crystalline layers to lamellar crystallites: a major route followed in polymer crystallization? *Eur. Phys. J. E* **2000**, *3*, 165–183.
14 Heck, B.; Hugel, T.; Iijima, M.; Strobl, G. Steps in the formation of the partially crystalline state. *Polymer* **2000**, *41*, 8839–8848.
15 Strobl, G. A thermodynamic multiphase scheme treating polymer crystallization and melting. *Eur. Phys. J. E* **2005**, *18*, 295–309.
16 Lv, Z. Y.; Zhang, M. C.; Zhang, Y.; Guo, B. H.; Xu, J. Study on melting and recrystallization of poly(butylene succinate) lamellar crystals *via* step heating differential scanning calorimetry. *Chinese J. Polym. Sci.* **2017**, *35*, 1552–1560.
17 Yao, S. F.; Chen, X. T.; Ye, H. M. Investigation of structure and crystallization behaviour of poly(butylene succinate) by Fourier transform infrared spectroscopy. *J. Phys. Chem. B* **2017**, *121*, 9476–9485.
18 Wei, Z. Y.; Yu, Y.; Zhou, C.; Zheng, L. C.; Leng, X. F.; Li, Y. Relationship between melting behaviour and morphological changes of semicrystalline polymers. *J. Therm. Anal. Calorim.* **2017**, *129*, 777–787.
19 Charlon, S.; Delbreilh, L.; Dargent, E.; Follain, N.; Soulestin, J.; Marais, S. Influence of crystallinity on the dielectric relaxations of poly(butylene succinate) and poly[(butylene succinate)-*co*-(butylene adipate)]. *Eur. Polym. J.* **2016**, *84*, 366–376.
20 Beckingham, B. S.; Ho, V.; Segalman, R. A. Formation of a rigid amorphous fraction in poly(3-(2'-ethyl)hexylthiophene). *ACS Macro. Lett.* **2014**, *3*, 684–688.
21 Wei, Z. Y.; Song, P.; Zhou, C.; Chen, G. Y.; Chang, Y.; Li, J. F.; Zhang, W. X.; Liang, J. C. Insight into the annealing peak and microstructural changes of poly(L-lactic acid) by annealing at elevated temperatures. *Polymer* **2013**, *54*, 3377–3384.
22 Bonnet, M.; Rogausch, K. D.; Petermann, J. The endothermic "annealing peak" of poly(phenylene sulphide) and poly(ethylene terephthalate). *Colloid Polym. Sci.* **1999**, *277*, 513–518.
23 Alizadeh, A.; Richardson, L.; Xu, J.; McCartney, S.; Marand, H.; Cheung, Y. W.; Chum, S. Influence of structural and topological constraints on the crystallization and melting behaviour of polymers 1. Ethylene/1-octene copolymers. *Macromolecules* **1999**, *32*, 6221–6235.
24 Marand, H.; Alizadeh, A.; Farmer, R.; Desai, R.; Velikov, V. Influence of structural and topological constraints on the crystallization and melting behaviour of polymers 2. Poly(arylene ether ether ketone). *Macromolecules* **2000**, *33*, 3392–3403.
25 Alizadeh, A.; Sohn, S.; Quinn, J.; Marand, H.; Shank, L. C.; Iler, H. D. Influence of structural and topological constraints on the crystallization and melting behaviour of polymers: 3. *Bisphenol A polycarbonate. Macromolecules* **2001**, *34*, 4066–4078.
26 Edling, H. E.; Vincent, M.; Marand, H.; Talley, S. J.; Barr, K.; Moore, R. B.; Turner, S. R. Synthesis and crystallization behaviour of rigid copolyesters with biphenyl-4,4'-dicarboxylate and 2,6-naphthalenedicarboxylate in the main chain. *J. Polym. Sci., Part B Polly. Phys.* **2019**, *57*, 973–980.
27 Furushima, Y.; Toda, A.; Rousseaux, V.; Bailly, C.; Zhuravlev, E.; Schick, C. Quantitative understanding of two distinct melting kinetics of an isothermally crystallized poly(ether ether ketone). *Polymer* **2016**, *99*, 97–104.
28 Jariyavidyanont, K.; Androsch, R.; Schick, C. Crystal reorganization of poly(butylene terephthalate). *Polymer* **2017**, *124*, 274–283.
29 Schulz, M.; Seidlitz, A.; Petzold, A.; Thurn-Albrecht, T. The effect of intracrystalline chain dynamics on melting and reorganization during heating in semicrystalline polymers. *Polymer* **2020**, *196*,

122441.
30 Ye, H. M.; Wang, R. D.; Liu, J.; Xu, J.; Guo, B. H. Isomorphism in poly(butylene succinate-*co*-butylene fumarate) and its application as polymeric nucleating agent for poly(butylene succinate). *Macromolecules* **2012**, *45*, 5667–5675.
31 Ye, H. M.; Chen, X. T.; Li, H. F.; Zhang, P.; Ma, W. Z.; Li, B. T.; Xu, J. Industrializable and sustainable approach for preparing extended-chain crystals of biodegradable poly(butylene succinate) and their applications. *Polymer* **2019**, *160*, 93–98.
32 Ye, H. M.; Chen, X. T.; Liu, P.; Wu, S. Y.; Jiang, Z. Y.; Xiong, B. J.; Xu, J. Preparation of poly(butylene succinate) crystals with exceptionally high melting point and crystallinity from its inclusion complex. *Macromolecules* **2017**, *50*, 5425–5433.
33 Ichikawa, Y.; Kondo, H.; Igarashi, Y.; Noguchi, K.; Okuyama, K.; Washiyama, J. Crystal structures of α and β forms of poly(tetramethylene succinate). *Polymer* **2000**, *41*, 4719–4727.
34 Ichikawa, Y.; Kondo, H.; Igarashi, Y.; Noguchi, K.; Okuyama, K.; Washiyama, J. Crystal structures of α and β forms of poly(tetramethylene succinate). *Polymer* **2001**, *42*, 847–847.
35 Liu, G. M.; Zheng, L. C.; Zhang, X. Q.; Li, C. C.; Wang, D. J. Critical stress for crystal transition in poly(butylene succinate)-based crystalline-amorphous multiblock copolymers. *Macromolecules* **2014**, *47*, 7533–7539.
36 Liu, G. M.; Zheng, L. C.; Zhang, X. Q.; Li, C. C.; Jiang, S. C.; Wang, D. J. Reversible lamellar thickening induced by crystal transition in poly(butylene succinate). *Macromolecules* **2012**, *45*, 5487–5493.
37 Nikolic, M. S.; Djonlagic, J. Synthesis and characterization of biodegradable poly(butylene succinate-*co*-butylene adipate)s. *Polym. Degrad. Stabil.* **2001**, *74*, 263–270.
38 Schmidtke, J.; Strobl, G.; ThurnAlbrecht, T. A four-state scheme for treating polymer crystallization and melting suggested by calorimetric and small angle X-ray scattering experiments on syndiotactic polypropylene. *Macromolecules* **1997**, *30*, 5804–5821.
39 Strobl, G. R.; Schneider, M. Direct evaluation of the electron-density correlation-function of partially crystalline polymers. *J. Polym. Sci., Part B: Polym. Phys.* **1980**, *18*, 1343–1359.
40 Zhang, S. J.; Han, J. R.; Gao, Y.; Guo, B. H.; Reiter, G.; Xu, J. Determination of the critical size of secondary nuclei on the lateral growth front of lamellar polymer crystals. *Macromolecules* **2019**, *52*, 7439–7447.
41 Xu, Y. X.; Xu, J.; Sun, Y. B.; Liu, D. H.; Guo, B. H.; Xie, X. M. Crystallization behaviour of poly(butylene succinate-*co*-propylene succinate)s. *Acta Polymerica Sinica* (in Chinese) **2006**, 1000–1006.
42 Yoo, E. S.; Im, S. S. Melting behaviour of poly(butylene succinate) during heating scan by DSC. *J. Polym. Sci., Part B: Polym. Phys.* **1999**, *37*, 1357–1366.
43 Wang, X. H.; Zhou, J. J.; Li, L. Multiple melting behaviour of poly(butylene succinate). *Eur. Polym. J.* **2007**, *43*, 3163–3170.
44 Yasuniwa, M.; Satou, T. Multiple melting behaviour of poly(butylene succinate). I. Thermal analysis of melt-crystallized samples. *J. Polym. Sci., Part B: Polym. Phys.* **2002**, *40*, 2411–2420.
45 Yasuniwa, M.; Tsubakihara, S.; Satou, T.; Iura, K. Multiple melting behaviour of poly(butylene succinate). II. Thermal analysis of isothermal crystallization and melting process. *J. Polym. Sci., Part B: Polym. Phys.* **2005**, *43*, 2039–2047.
46 Phillips, P. J.; Rensch, G. J. Crystallization studies of poly(epsilon-caprolactone). 2. Lamellar thickening and melting. *J. Polym. Sci., Part B: Polym. Phys.* **1989**, *27*, 155–173.
47 Cheng, S. Z. D.; Chen, J. H.; Barley, J. S.; Zhang, A. Q.; Habenschuss, A.; Zschack, P. R. Isothermal thickening and thinning processes in low-molecular-weight poly(ethylene oxide) fractions crystallized from the melt. 3. Molecular-weight dependence. *Macromolecules* **1992**, *25*, 1453–1460.
48 Marand, H.; Huang, Z. Y. Isothermal lamellar thickening in linear polyethylene: correlation between the evolution of the degree of crystallinity and the melting temperature. *Macromolecules* **2004**, *37*, 6492–6497.
49 Lee, Y. C.; Porter, R. S. Double-melting behaviour of poly(ether ether ketone). *Macromolecules* **1987**, *20*, 1336–1341.
50 Zhuravlev, E.; Schmelzer, J. W. P.; Wunderlich, B.; Schick, C. Kinetics of nucleation and crystallization in poly(epsilon-caprolactone) (PCL). *Polymer* **2011**, *52*, 1983–1997.
51 Furushima, Y.; Nakada, M.; Ishikiriyama, K.; Toda, A.; Androsch, R.; Zhuravlev, E.; Schick, C. Two crystal populations with different melting/reorganization kinetics of isothermally crystallized polyamide 6. *J. Polym. Sci., Part B: Polym. Phys.* **2016**, *54*, 2126–2138.
52 Konishi, T.; Sakatsuji, W.; Fukao, K.; Miyamoto, Y. Temperature dependence of lamellar thickness in isothermally crystallized poly(butylene terephthalate). *Macromolecules* **2016**, *49*, 2272–2280.
53 Furushima, Y.; Nakada, M.; Yoshida, Y.; Okada, K. Crystallization/melting kinetics and morphological analysis of polyphenylene sulfide. *Macromol. Chem. Phys.* **2018**, *219*, 7.
54 Strobl, G. *The physics of polymers*. Springer-Verlag, New York, **1997**.
55 Doye, J. P. K.; Frenkel, D. Mechanism of thickness determination in polymer crystals. *Phys. Rev. Lett.* **1998**, *81*, 2160–2163.
56 Rottele, A.; Thurn-Albrecht, T.; Sommer, J. U.; Reiter, G. Thermodynamics of formation, reorganization, and melting of confined nanometer-sized polymer crystals. *Macromolecules* **2003**, *36*, 1257–1260.

https://doi.org/10.1007/s10118-021-2530-2